Electrodeposition and Corrosion Resistance of Zn-Pd Alloy from the $ZnCl_2$-EMIC(1-ethyl-3-methylimidazolium chloride)-$PdCl_2$ Room Temperature Molten Salt

Hsin-Yi Hsu and Chao-Chen Yang

Department of General Education, The Overseas Chinese Institute of Technology, 100 Chiao-Kwang Road, Taichung 407, Taiwan, R. O. C.

Reprint requests to Prof. C.-C. Yang. E-mail: yangcc@flame.yuntech.edu.tw. Fax: 886-5-531-2056

Z. Naturforsch. **58b,** 1055 – 1062 (2003); received May 9, 2003

Electric conductivities of 50-50 mol% $ZnCl_2$-EMIC and its mixtures with 0.6714 mol% $PdCl_2$ room-temperature molten salts (RTMS) have been measured by a computerized system based on a d.c. four-probe method. The conductivity of the former is greater than that of the latter. These conductivities are well fitted by Arrhenius equations and the activation energies are calculated to be 25.22 and 26.28 kJ/mol, respectively. Cyclic voltammetry for the $ZnCl_2$-EMIC-$PdCl_2$ melt has been performed on Pt and Cu working electrodes. The cathodic reduction waves of Pd^{2+} and Zn^{2+} species and the oxidation waves for Zn-Pd alloys rich in Zn and Pd have been observed for the cyclic voltammograms on the Pt working electrode. The deposition potentials have been measured to be -0.7 V and -1.3 V on the Cu substrate. The morphology and composition of the electrodeposited layers obtained under different conditions have been analyzed by SEM and EDS, respectively; layers with a finer (about 300 – 500 nm), denser and higher Pd content have been obtained by pulse plating on the Cu sheet at t_{on}/t_{off} = 3/1 under -0.7 V at 80 °C. The XRD patterns also reveal that the structure of these deposited layers can be regarded as amorphous. Tafel polarization curves of the electrodeposited layers in 3.5 wt% NaCl solution have been drawn. The results indicate that the Zn-Pd alloy deposits have much higher corrosion resistance and protection efficiency than the Zn-deposited layer; the corrosion potentials shift positively by about 700 $\sim$ 950 mV. Furthermore, the pulse plating has a better performance than the direct current plating, and the reason is discussed.

Key words: Room Temperature Molten Salt, Cyclic Voltammetry, Electrodeposition, Corrosion Resistance

Introduction

In recent years, many new materials have been developed for engineering applications, but steel is sill used as the main construction material for automobiles, appliances and industrial machinery. A large amount of steel is consumed in a wide range of applications, but owing to its susceptibility to corrosion, steel is nearly always used with a protective coating. Zinc metal has excellent corrosion resistance in neutral water and a lower corrosion potential than steel plates have. The property which gives zinc this valuable resistance comes from its ability to form a protective layer composed of zinc oxide and hydroxide or different basic salts depending on the nature of the environment. These corrosion products provide some degree of barrier protection against corrosion, giving Zn-coated steel better corrosion resistance than the bare plates. The corrosion protection of galvanized steels arises from the barrier action of a zinc layer, the secondary barrier action of the zinc corrosion products, and the cathodic protection of zinc with the coating acting as a sacrificial anode. Therefore, zinc finds wide and varied applications especially as a metal coating for the prevention of corrosion of steel fabrications exposed to water.

Zinc and its alloys are widely used for corrosion protection of steel. Alloy coatings appear to be particularly attractive, since under similar electroplating conditions these deposits exhibit better corrosion resistance and physical properties than a pure zinc layer. Recent developments to increase the corrosion resistance include the use of Zn-alloys using Ni [1, 2], Co [3 – 6], Cu [7], Al [8], Cr [9], Mn [10], Fe [11], In [12] and rare earth metals [13]. It is generally assumed that Zn-alloy coatings with a low concentration of an alloying element can provide big improvements in corrosion resistance. Thus, alloying seems to be the

0932–0776 / 03 / 1100–1055 $ 06.00

most important approach in the field of corrosion resistance. According to the above-mentioned research reports, electrodeposited zinc alloys are good materials for highly corrosion-resistant coatings, and the electrodepositions are normally performed in aqueous electrolyte solutions, where there are some problems, however, with hydrogen embrittlement and small current efficiency. To overcome these problems, molten salts may be considered, which are aprotic solvents and possess some unique properties, *e. g.*, high conductivity, a wide electrochemical window and low vapor pressure. It is somewhat difficult, however, to use conventional molten salts which have to be treated at high temperatures with special apparatus. On the other hand, the melting points of RTMS are low and therefore the handling is easier. Sun *et al.* [6, 7] have studied the electrodeposition of Zn, Zn-Co and Zn-Cu alloys from acidic $ZnCl_2$-EMIC RTMS (EMIC = 1-ethyl-3-methylimidazolium chloride). However, the conductivities of such mixed melts have not been reported. The electrochemistry of such an electrodeposition of a Zn-Pd alloy from acidic $ZnCl_2$-EMIC melts has not been investigated, either.

Palladium possesses some excellent characteristics, such as corrosion resistance, hydrogen adsorption and catalysis of chemical reactions, which have received considerable attention. Bell *et al.* [14, 15] developed a palladium-modified thermal oxidation (PTO) to improve the corrosion and wear resistance of titanium. Skeldon *et al.* [16] reported that corrosion protection of titanium as an electron-transparent window material can be improved by pulsed plasma deposition of palladium. Palladium-based membranes have been the focus of many studies because of their potential in hydrogen purification or membrane reactors including catalytic dehydrogenation reactions. Lee *et al.* [17,18] reported the preparation of a Pd-Ni alloy membrane deposited on a porous stainless steel support by vacuum electodeposition for hydrogen separation. Higuchi *et al.* [19] also reported that a three-layered Pd/Mg/Pd thin film shows some remarkable hydrogen storage properties. Porte *et al.* [20] studied the catalytic activity of palladium thin layers deposited on a Ni(110) surface for the hydrogenation reaction of 1,3-butadiene. Alloying materials have been the subject of numerous recent studies, since these have particular characteristics as compared with traditional metals, especially regarding the corrosion resistance, catalytic properties and magnetism. These properties have so far not been reported for Zn-Pd alloys electrodeposited from the RTMS. In the present work, electrodeposition and corrosion resistance of a Zn-Pd alloy generated from the 50-50 mol% $ZnCl_2$-EMIC RTMS containing a small amount of $PdCl_2$ (0.6714 mol%) were investigated; these melts will be hereafter abbreviated as ZE and ZEP, respectively.

A study on the catalytic property and the hydrogen separation performance of the Zn-Pd alloy, however, still remain to be investigated.

Besides, the electrochemistry and nucleation mechanism of palladium chloride in acidic ZE has been investigated by cyclic voltammetry and chronoamperometry, respectively. The electrodepositions of Zn-Pd alloys have been performed on a Cu substrate by controlled potential coulometry and pulse plating, and the morphology, composition and corrosion behavior of the electrodeposited layers have been analyzed by SEM (scanning electron microscopy), EDS (energy dispersive X-ray spectroscopy) and Tafel polarization curves, respectively.

Experimental Section

$ZnCl_2$ (Merck, anhydrous, 98%), EMIC (1-ethyl-3-methylimidazolium chloride, Aldrich, 98%), and $PdCl_2$ (Lancaster, 99%) were used as received. The ZEP was prepared by continuous stirring for 12 h under a purified nitrogen atmosphere in a glove box. The electrical conductivity of the melts was measured by a computerized system for a d.c. four-probe method described previously [21].

The electrochemical experiments were performed in a sealed three-electrode electrochemical cell. Platinum or copper (geometric area: 0.1571 cm^2) working electrodes were made by winding a Teflon tape around Pt and Cu rods (Nilaco, 99.99%), respectively, and inserting these into a glass tube. The electrodes were polished successively with increasingly finer grades of emery papers, finally followed by rinsing with acetone and distilled water, and dried under a vacuum. The counter electrode was a zinc spiral (Nilaco, 99.9%) connected to a Pt wire sealed in a glass tube and immersed in the bulk electrolyte melt. The reference electrode was also a zinc wire immersed in the ZE contained in a sealed Pt wire glass tube. The electrochemical behavior and the nucleation mechanism of the melts were studied on the Pt or Cu electrode by cyclic voltammetry and chronoamperometry, respectively, with an EG&G model 273A potentiostat/galvanostat controlled with an EG&G model 270/250 software.

Electrodeposition of the amorphous Zn-Pd alloys was performed at different deposition potentials and current densities by controlled potential coulometry and pulse plating. For all of the deposition experiments, a fixed amount of electric-

Table 1. Parameters for the electrical conductivity equation of the ZE and ZEP. As for ZE and ZEP, see the text: $\sigma = a + bt + ct^2$.

Melt component	$a/10^{-2}$ S·cm^{-1}	$b/10^{-4}$ S·cm^{-1}	$c/10^{-6}$ S·cm^{-1}	R squared	t/°C
ZE	−0.996	1.4594	1.8778	0.9994	70 – 150
ZEP	−0.2899	0.0477	2.3342	0.9994	64 – 150

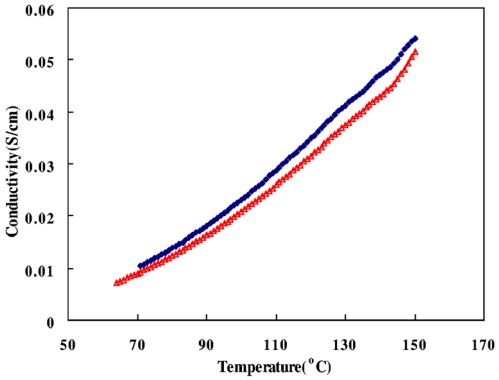

Fig. 1. The conductivities of the ZE and ZEP as a function of the temperature. As for ZE and ZEP, see the text. ♦: ZE; △: ZEP.

ity was passed to make the comparison easier. At the end of the experiment, the electrodes were taken out from the molten electrolytes, washed with dry propylene carbonate, ethanol, and deionized water and, after slight supersonic rinsing, dried and stored in a desiccator for further analysis. The morphology and composition of the electrodeposited layers were determined by SEM and EDS, respectively. The structure of the deposited layers was analyzed by an X-ray diffractometer (Shimadzu, Cu-K$_\alpha$). The corrosion behavior of the electrodeposited layer was also analyzed by Tafel polarization curves.

Results and Discussion

The conductivities of the ZE and ZEP melts are shown as a function of temperature in Fig. 1. The experimental data were least-squares fitted to equations of a form $\sigma = a + bt + ct^2$, where t is the temperature in °C. The obtained parameters a, b and c are given in Table 1. As the squared R values are larger than 0.998, the above equations fit the experimental data very well. Fig. 1 shows that the conductivities of the two melts increase nearly linearly with temperature, and that the conductivity of ZE is greater than that of ZEP. The results may be explained in terms of the complex formation. Formation of palladium complex ions appears to be easy and to reduce the mobility of the

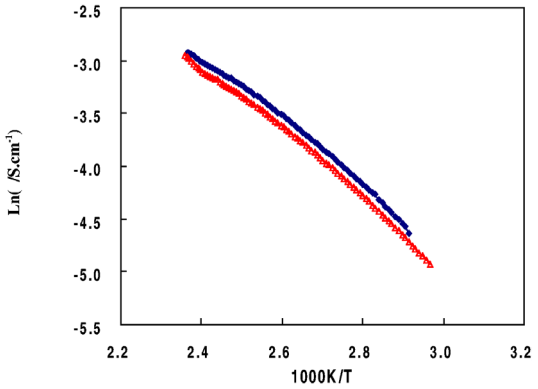

Fig. 2. Arrhenius plots of the electrical conductivity for the ZE and ZEP. As for ZE and ZEP, see the text. ♦: ZE; △: ZEP.

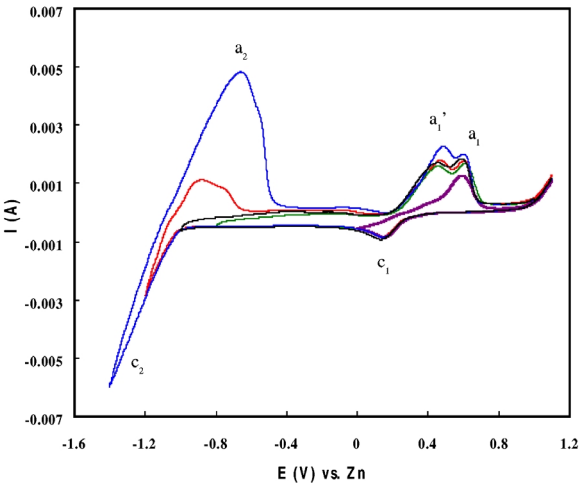

Fig. 3. Cyclic voltammograms for the ZEP melt on the Pt electrode at 80 °C under different scan reverses. Scan rate: 50 mV/s.

ions in the melt. The conductivity of the melt containing $PdCl_2$ will therefore decrease. Do our best knowledge, the paper about the study of ionic reaction for ZEP melt has not been published. So, the Raman spectrum analysis of ZEP melt will be next research. These conductivities were fitted by the Arrhenius equation [22 – 25].

$$\sigma = \sigma_0 \exp(-E_a/RT) \quad (1)$$

Plots of the data for the ZE and ZEP are shown in Fig. 2. The result reveals that an Arrhenius equation is also quite well obeyed over the temperature range studied. The activation energies (E_a) are calculated to

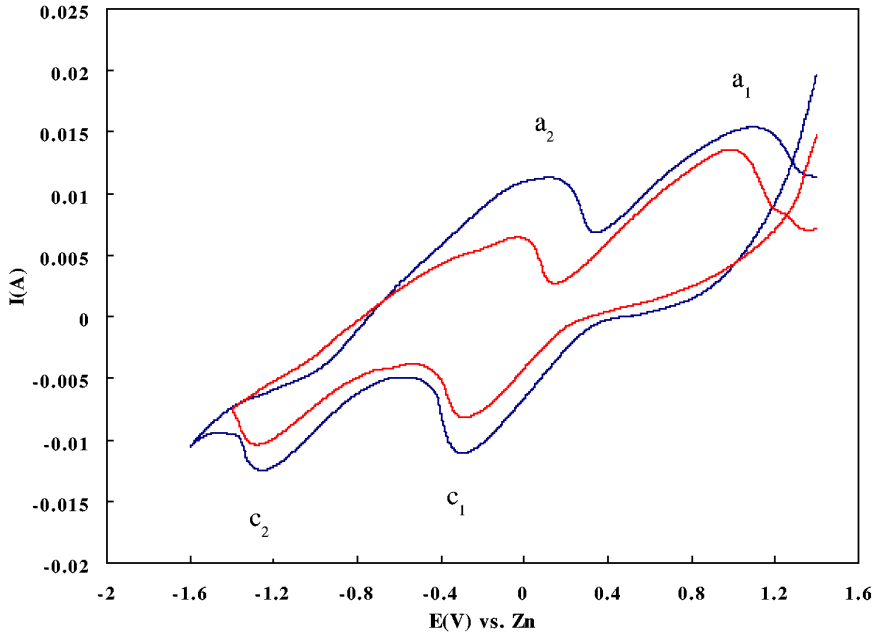

Fig. 4. Cyclic voltammograms for the ZEP melt on the Cu electrode at 80 °C under different scan reverses. Scan rate: 50 mV/s.

be 25.22 and 26.28 kJ/mol for the ZE and ZEP, respectively.

The electrochemical behavior of palladium chloride in ZE on different working electrodes has been investigated by cyclic voltammetry. The cyclic voltammograms for the ZEP on the Pt working electrode at 80 °C under different scan reverses are shown in Fig. 3. These voltammograms exhibit two reduction waves (c_1,c_2), two major oxidation waves (a_1,a_2) and a secondary oxidation wave (a_1'). The two reduction waves must be due to the cathodic reduction of Pd^{2+} (wave c_1, about 0.15 V) and Zn^{2+} species (wave c_2). Figure 3 also exhibits a stripping wave (a_2) of the zinc deposit. The one observed in the voltammograms of the ZEP is not as sharp as for ZE. Based on this observation, it is assumed that the Zn-Pd alloy is electrodeposited and the wave a_2 is attributed to the oxidation of the Zn-Pd alloy deposit rich in Zn. Moreover, it is observed that the oxidation wave a_1' disappears as the scan reverse is set to 0 V. This indicates that the oxidation wave a_1 (about 0.6 V) must be due to the anodic stripping of Pd that was electrodeposited on the Pt electrode at wave c_1 (0.15 V); therefore, wave a_1' must be due to oxidation of the Zn-Pd alloy deposit rich in Pd.

Figure 4 shows the cyclic voltammograms for the ZEP on the Cu electrode at 80 °C under two scan reverses. There are two reduction waves (c_1,c_2) and two oxidation waves (a_1, a_2). The wave c_2 must be due to the reduction of Zn^{2+} species and the wave a_2 must be the associated oxidation wave. Moreover, the wave c_1 must be due to the reduction of Pd^{2+} species and the wave a_1 must be the associated oxidation wave. The results in Fig. 4 show that the waves c_1 and c_2 are at *ca.* −0.3 V and −1.3 V, respectively. Cyclic voltammetry on the Cu substrate has been performed six times successively; the result is shown in Fig. 5. It shows that the wave c_1 shifts to more negative poten-

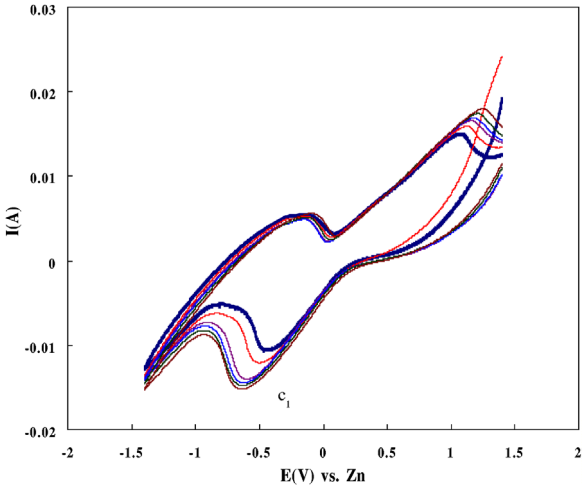

Fig. 5. Cyclic voltammograms with six times successively for the ZEP melt on the Cu electrode at 80 °C. Scan rate: 50 mV/s.

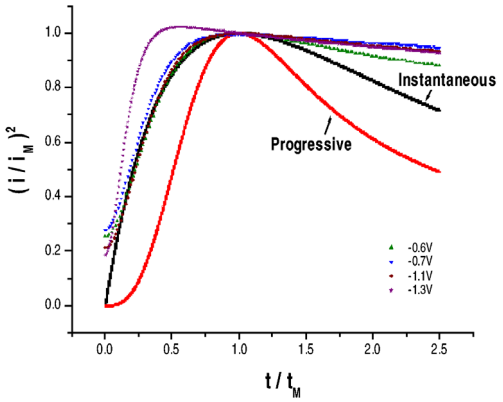

Fig. 6. Reduced-variable plots of current-time transients obtained with the ZEP melt on the Cu electrode at 80 °C. Theoretical curves for instantaneous and progressive nucleation are also shown for comparison.

tial (*ca.* −0.7 V), which reveals that the Zn-Pd alloy may have survived on the Cu substrate surface. Based on the observation, the deposition potentials have been evaluated to be −0.7 V and −1.3 V on the Cu substrate.

In order to investigate the alloy nucleation/growth process, chronoamperometry was carried out on the Cu electrode. Reduced-variable plots shown in Fig. 6 have been derived from the current-time transients, which enable us to compare the results with the standard model for three-dimensional instantaneous and progressive nucleation [26]. The dimensionless experimental current-time transients resulted from chronoamperometry for the deposition of the alloy from the ZEP on the Cu substrate.

Figure 6 reveals that for the alloy electrodeposition on the Cu electrode the nucleation is an instantaneous one; however, it is conjectured that, as the applied deposition potential becomes more negative (−1.3 V), the nucleation density increases, which, in turn, rapidly shortens the time required for the diffusion zones to overlap. In other words, the diffusion current will more rapidly reach the Cottrell current [27].

The Zn-Pd alloy was electrodeposited under different electrodeposition conditions on a Cu sheet at 80 °C from the ZEP. The compositions of the electrodeposits are given in Table 2, which indicate that a less negative potential (−0.7 V) or lower current density (−4.46 mA/cm^2) are more advantageous to the electrodeposition of the Pd component (Fig. 4). Furthermore, when the applied deposition potential is more negative (−1.3 V), the Zn content of the electrodeposits is above 90 atom%.

Table 2. The compositions and electrodeposition conditions of electrodeposited layers shown in Fig. 7, which were analyzed by EDS.

Sample	Composition(atom%) Zn	Pd	Electrodeposition conditions
a	45.74	54.26	−0.7 V, potentiostatic, direct current, 40 °C
b	92.93	7.07	−1.3 V, potentiostatic, direct current, 40 °C
c	56.1	43.9	−0.7 V, potentiostatic, pulse current (3:1), 40 °C
d	92.04	7.96	−1.3 V, potentiostatic, pulse current(3:1), 40 °C
e	75.91	24.09	−4.46 mA/cm^2, galvanostatic, pulse current (3:1), 40 °C
f	90.08	9.92	−17.86 mA/cm^2, galvanostatic, pulse current (3:1), 40 °C

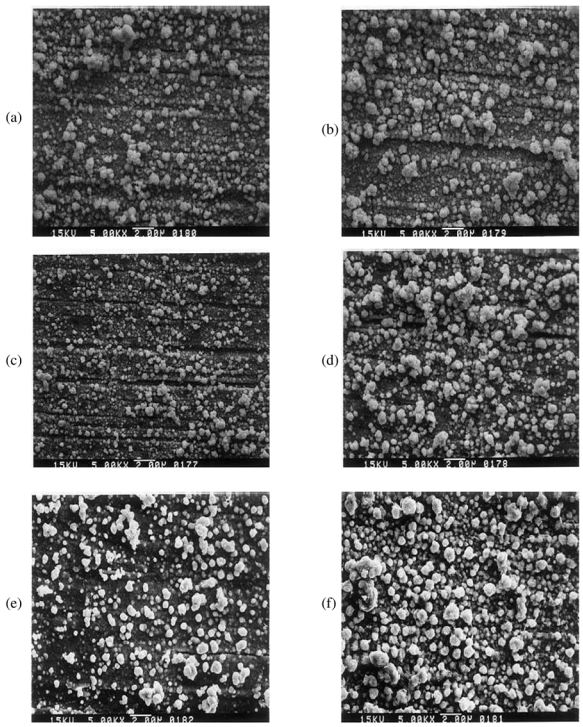

Fig. 7. SEM micrographs of Zn-Pd layers electrodeposited from the ZEP melt on the Cu sheet at 80 °C. The electrodeposition conditions were shown as in Table 2.

The SEM micrographs of the layers electrodeposited under different conditions from the ZEP on the Cu sheet are shown in Fig. 7. This reveals that the surface morphologies are similar, and that all deposits possess about 300 ∼ 1000 nm particle struc-

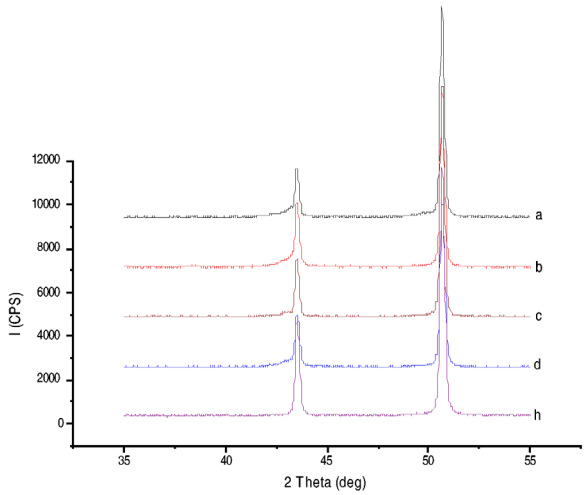

Fig. 8. XRD patterns of Zn-Pd layers electrodeposited from the ZEP melt on the Cu sheet at 80 °C. The sample a, b, c, and d were shown as in Table 2, and sample h is pure Cu.

ture. However, it is obvious that layers with a finer (about 300 ∼ 500 nm), denser and higher Pd content are deposited with the pulse plating on the Cu sheet at t_{on}/t_{off} = 3/1 under −0.7 V at 80 °C, as shown in Fig. 7(c). The result may be explained in terms of the effect of pulse plating.

For a pulse electrodeposition process, the crystallization of the electrodeposited layer is a very important step for the electrogrowth, since it influences directly the structure of the deposit and therefore its properties. The crystallization is a process by which the adatoms or adions are incorporated in the crystal lattice. Crystallization occurs either by the build-up of old crystals or by the formation and growth of new ones. These two processes are in competition and can be influenced by different factors. High surface diffusion rates, low population of adatoms, and low over-potentials are factors enhancing the build-up of old crystals. On the contrary, low surface diffusion rates, high population of adatoms and high over-potentials on the surface enhance the creation of new nuclei. Since in the pulse current electrodeposition the pulse current density is usually considerably higher than the corresponding direct current density, the population of adatoms on the surface during pulse electrodeposition is higher than during direct current electrodeposition, resulting in an increased nucleation rate and a more finely grained structure.

Table 3. Corrosion potential (E_{corr}), corrosion current density (I_{corr}) and protection efficiency of the samples in 3.5 wt% NaCl solution. The sample a, b, c, d, e, and f were shown as in Table 2; sample i, h, and g are pure Zn, pure Cu and Zn-deposited layer, respectively.

Sample	E_{corr} (V/Ag/AgCl)	I_{corr} (μA/cm^2)	Protection efficiency, η (%)
a	−0.0537	117.6	65.57
b	−0.3046	288.1	15.66
c	−0.1086	24.24	92.90
d	−0.2525	125.2	63.35
e	−0.1246	80.41	76.46
f	−0.1915	70.59	79.34
g	−1.011	341.6, $(I_{corr})_0$	–
h (Cu)	−0.1793	54.1	–
i (Zn)	−0.9936	146.1	–

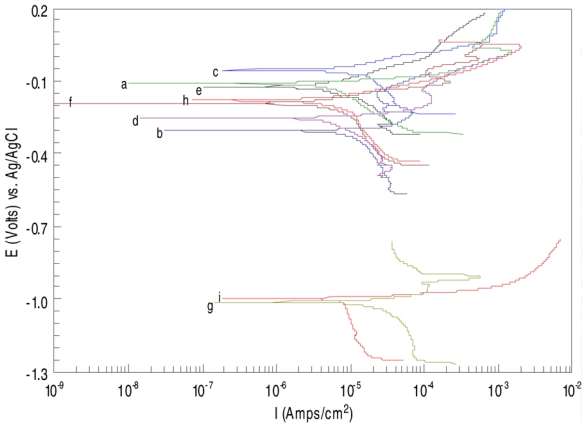

Fig. 9. Tafel polarization curves of Zn-Pd electrodeposited layers in 3.5 wt% NaCl solution. The sample a, b, c, d, e, and f were shown as in Table 2; sample i, h, and g are pure Zn, pure Cu, and Zn-deposited layer, respectively.

X-ray diffraction patterns of the deposited layers are shown in Fig. 8. It is observed that the XRD patterns of the layers electrodeposited under different conditions are similar to the pattern of the pure Cu, but there are no other obvious peaks. This indicates that the structure of these deposited layers can be regarded as amorphous.

Tafel plots of E (potential) versus log I (current density) for pure Cu, pure Zn and the electrodeposited layers in 3.5 wt% NaCl solution are shown in Fig. 9. It is obvious that the corrosion potentials of the layers electrodeposited under different conditions are shifted (about 700 ∼ 950 mV) positively, as compared to the pure Zn and Zn-deposited layer. The result indicates that the Zn-Pd alloy deposit has a very good corro-

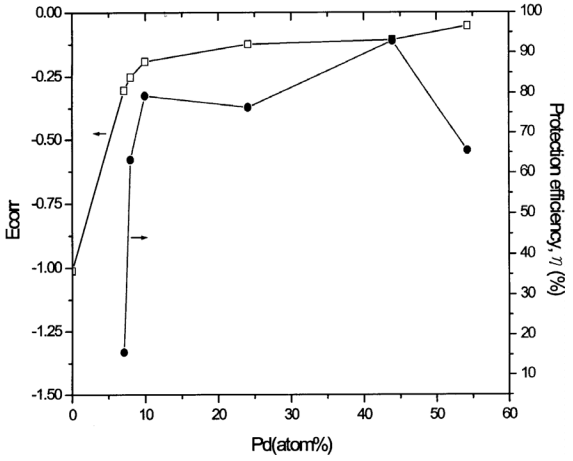

Fig. 10. Relationships between the E_{corr} or protecion efficiancy (η) and the Pd content (atom%) of electrodeposited layers.

sion resistance compared with the pure Zn and Zn-deposited layer. Moreover, it should be noted that the corrosion potentials of samples a, c and e exhibit a better corrosion resistance than pure Cu. Besides, the anodic polarization of these electrodeposited layers shows multi-step reactions, indicating that the deposited layer has protected the substrate from corrosion, resulting in the lower anodic corrosion current density of these samples, as compared to pure Cu or Zn. However, the criteria for good protection performance may be the values of corrosion potential (E_{corr}) and corrosion current density (I_{corr}) of the sample under given environments. The results of these samples in 3.5 wt% NaCl solution are given in Table 3. The protection efficiency (η %) of the sample is estimated using formula (2),

$$\eta = \frac{(I_{\text{corr}})_{\text{o}} - I_{\text{corr}}}{(I_{\text{corr}})_{\text{o}}} \times 100 \qquad (2)$$

where $(I_{\text{corr}})_{\text{o}}$ is the corrosion current density of a Zn-deposited layer on the Cu substrate. Due to the formation of the amorphous Zn-Pd alloy layer, the corrosion current density declines considerably as compared with the Zn-deposited layer, suggesting that the protection efficiency of the Zn-Pd alloy may reach above 63% excluding sample b.

Figure 10 shows the relationship between E_{corr} or the protection efficiency (η) and the Pd content (atom%). It is observed that E_{corr} has much improved as the Pd content is smaller than 8 atom%; on the other hand, the E_{corr} tardily increases, as the Pd content is above 8 atom%, indicating that the protection efficiency may reach as high as 93%. It is noted that sample b obtained with direct current plating has a lower protection efficiency than the other samples obtained with pulse plating. It is conjectured that the pulse plating method can produce a more densely deposited layer, as compared with the direct current plating.

Conclusions

The conductivity of ZE is greater than that of ZEP. The result may be explained in terms of complex formation which is readily achieved for palladium. The resulting melt reduces the mobility of the ions in the melt. Moreover, these conductivities are well fitted by the Arrhenius equation and the activation energies are calculated to be 25.22 and 26.28 kJ/mol for the ZE and ZEP melts.

In the cyclic voltammograms of the Pt working electrode, the cathodic reduction waves of Pd^{2+} and Zn^{2+} species and the oxidation waves of the Zn-Pd alloys rich both in Zn and Pd have been observed. Moreover, in the cyclic voltammograms of the Cu working electrode, the reduction and oxidation waves of Pd^{2+} and Zn^{2+} species are also detected.

The morphology and composition of the layers electrodeposited under different conditions have been analyzed by SEM and EDS, respectively. Layers with a finer (about 300 $\sim$ 500 nm), denser and higher Pd content have been deposited with the pulse plating on the Cu sheet at $t_{\text{on}}/t_{\text{off}}$ = 3/1 under -0.7 V at 80 °C. Furthermore, the XRD patterns have revealed that the structure of these layers can be regarded as amorphous.

Tafel polarization curves of the electrodeposited layers in 3.5 wt% NaCl solution have been drawn. The result indicates that the Zn-Pd alloy deposit has a very good corrosion resistance compared with the pure Zn and Zn-deposited layer; the corrosion potentials shift positively by about 700 $\sim$ 950 mV. Moreover, the corrosion current density declines considerably compared to the Zn-deposited layer, and the protection efficiency is much improved owing to the formation of an amorphous Zn-Pd alloy by pulse plating. The pulse plating has a better performance than the direct current plating.

[1] C. Bowden, A. Matthews, Surf. Coat. Technol. **76/77**, 508 (1995).
[2] E. Beltowska-Lehman, P. Ozga, Z. Swiatek, C. Lupi, Surf. Coat. Technol. **151 – 152**, 444 (2002).
[3] J. Giridhar, W. J. van Ooij, Surf. Coat. Technol. **52**, 17 (1992).
[4] N. Koura, T. Endo, Y. Idemoto, J. Non-Cryst. Solids **205 – 207**, 650 (1996).
[5] N. Boshkov, K. Petrov, S. Vitkova, S. Nemska, G. Raichevsky, Surf. Coat. Technol. **157**, 171 (2002).
[6] P.-Y. Chen, I.-W. Sun, Electrochim. Acta **46**, 1169 (2001).
[7] P.-Y. Chen, M.-C. Lin, I.-W. Sun, J. Electrochem. Soc. **147(9)**, 3350 (2000).
[8] H. C. Shih, J. W. Hsu, C. N. Sun, S. C. Chung, Surf. Coat. Technol. **150**, 70 (2002).
[9] L. Guzman, M. Adami, W. Gissler, S. Klose, S. De Rossi, Surf. Coat. Technol. **125**, 218 (2002).
[10] B. Bozzini, E. Griskonis, A. Fanigliulo, A. Sulcius, Surf. Coat. Technol. **154**, 294 (2002).
[11] F. Y. Ge, S. K. Xu, S. B. Yao, S. M. Zhou, Surf. Coat. Technol. **88**, 1 (1996).
[12] J. M. Wang, Y. Lu, J. Zhang, C. Cao, Corros. Sci. **40**, 1161 (1998).
[13] A. Amadeh, B. Pahlevani, S. Heshmati-Manesh, Corros. Sci. **44**, 2321 (2002).
[14] A. Bloyce, P.-Y. Qi, H. Dong, T. Bell, Surf. Coat. Technol. **107**, 125 (1998).
[15] P.-Y. Qi, X.Y. Li, H. Dong, T. Bell, Mater. Sci. Eng. **A 326**, 330 (2002).
[16] S. D. Barson, P. Skeldon, G. E. Thompson, J. Piekoszewski, A. G. Chmielewski, Z. Werner, R. Grötzschel, E. Wieser, Corros. Sci. **42**, 1213 (2000).
[17] S.-E. Nam, S.-H. Lee, K.-H. Lee, J. Membr. Sci. **153**, 163 (1999).
[18] S.-E. Nam, K.-H. Lee, J. Membr. Sci. **170**, 91 (2000).
[19] K. Higuchi, K. Yamamoto, H. Kajioka, K. Toiyama, M. Honda, S. Orimo, H. Fujii, J. Alloys Compd. **330 – 332**, 526 (2002).
[20] L. Porte, M. Phaner-Goutorbe, J. M. Guigner, J. C. Bertolini, Surf. Sci. **424**, 262 (1999).
[21] H.-Y. Hsu, C.-C. Yang, Z. Naturforsch. **56a**, 670 (2001).
[22] R. A. Carpio, L. A. King, F. C. Kibler, Jr., A. A. Fannin, Jr., J. Electrochem. Soc. **126**, 1650 (1979).
[23] K. Ito, N. Nishina, H. Ohno, Electrochim. Acta **45**, 1295 (2000).
[24] J. D. Edwards, C. S. Taylor, A. S. Russell, L. F. Maranville, J. Electrochem. Soc. **90**, 527 (1952).
[25] H. Every, A. G. Bishop, M. Forsyth, D. R. MacFarlane, Electrochim. Acta **45**, 1279 (2000).
[26] B. Scharitfker, G. Hills, Electrochim. Acta **28**, 879 (1983).
[27] A. J. Bard, L. R. Faulkner, Electrochemical Methods; Fundamentals and Applications, John Wiley & Sons, New York (1980).